UKAEA-CCFE-CP(18)11

Yu.V. Yakovenko, V.V. Lutsenko, B.S. Lepiavko, V.Ya. Goloborodko, Ya.I. Kolesnichenko, A.I. Tishchenko, V. Kiptily, S. Sharapov, L. Giacomelli, T. Craciunescu, H. Weisen, JET Contributors

SIMULATIONS OF THE SAWTOOTH-INDUCED REDISTRIBUTION OF FAST IONS IN JET AND ITER

SIMULATIONS OF THE SAWTOOTH-INDUCED REDISTRIBUTION OF FAST IONS IN JET AND ITER

Yu.V. Yakovenko, V.V. Lutsenko, B.S. Lepiavko, V.Ya. Goloborodko, Ya.I. Kolesnichenko, A.I. Tishchenko, V. Kiptily, S. Sharapov, L. Giacomelli, T. Craciunescu, H. Weisen, JET Contributors

This paper has been submitted to
27th IAEA Fusion Energy Conference, Ahmedabad, India, 22-27 October 2018

SIMULATIONS OF THE SAWTOOTH-INDUCED REDISTRIBUTION OF FAST IONS IN JET AND ITER

Yu.V. YAKOVENKO, V.V. LUTSENKO, B.S. LEPIAVKO, V.Ya. GOLOBORODKO,
Ya.I. KOLESNICHENKO
Institute for Nuclear Research
Kyiv, Ukraine
Email: yyakovenko58@gmail.com

A.I. TISHCHENKO
National University of Kyiv Mohyla Academy
Kyiv, Ukraine

V. KIPTILY, S. SHARAPOV
Culham Centre for Fusion Energy
Abingdon, United Kingdom

L. GIACOMELLI
Department of Physics "G. Occhialini," University of Milano Bicocca
Milano, Italy

T. CRACIUNESCU
EURATOM-MedC Association, National Institute for Laser, Plasma and Radiation Physics
Bucharest, Romania

H. WEISEN
Swiss Plasma Center, École Polytechnique Fédérale de Lausanne
Lausanne, Switzerland

JET CONTRIBUTORS[1]

Abstract

Results of simulations of the sawtooth-induced redistribution of fast ions in JET and ITER with the code OFSEF are presented. The dependence of the redistribution on the particle parameters (energy and pitch angle) is studied. The redistribution of the trapped and marginally passing particles is found to exhibit barrier-like behaviour at the separatrix between the trapped and passing particles: the particles with high energies cannot pass the radial coordinate corresponding to the separatrix. The algorithm and structure of the rapid code developed on the basis of the OFSEF calculations are discussed. Simulations of the sawtooth effect on fusion alpha particles in ITER are carried out; they show that when the shape of the q-profile is non-parabolic (which is expected, for example, in the hybrid mode), the post-crash radial profile of the alpha particle distribution function can change significantly. Determining the parameters of a sawtooth crash – the sawtooth mixing radius and the sawtooth crash duration – from observations of the electron cyclotron emission in the equatorial plane of a tokamak is discussed; examples for JET sawtooth crashes are presented. Experimental observations of the sawtooth effect on the neutron emission in several recent JET discharges are presented and analysed.

1. INTRODUCTION

The sawtooth oscillations [1] are a widespread type of magnetohydrodynamic activity in tokamak plasmas. In TFTR, significant redistribution of fusion alpha particles by sawtooth oscillations was observed [2]. Sawtooth-induced redistribution of fast ions arising due to plasma heating was observed in many tokamaks (see, e.g., [3–5]). This shows that being able to simulate the effect of sawtooth oscillations on fast ions is important for predicting the performance of fusion reactors. Both theory [6] and recent experiments on DIII-D and ASDEX Upgrade [4, 7, 8] evidence that this effect depends on the particle energy and pitch angle. The aims of our research presented in the paper are to use JET experimental data for the verification of the available theory of the sawtooth-induced fast-ion redistribution, to develop new codes for simulations and diagnostics of sawtooth crashes, and to carry out predictive calculations of the sawtooth effect on alpha particles in ITER.

---

[1] See the author list of "X. Litaudon et al 2017 Nucl. Fusion 57 102001″

2. SIMULATIONS OF THE REDISTRIBUTION AND DEVELOPMENT OF A RAPID CODE

Simulations of the sawtooth-induced redistribution of fast deuterons in JET with the code OFSEF [8], which simulates the fast ion motion in the crash electromagnetic field, were carried out. The simulations had two aims: first, studying the dependence of the redistribution on the particle parameters; second, the development of a new rapid code for simulating the sawtooth effect on fast ions together with balance codes or even in real time.

The OFSEF simulations show that the well-passing ions (i.e., the ions with pitch angles sufficiently far from the separatrix with trapped particles) are redistributed by sawtooth crashes even at MeV energies. Low-energy particles are also strongly redistributed, the post-crash radial profiles of the distribution function weakly depending on the pitch angle. The redistribution of the trapped and marginally passing particles exhibits barrier-like behaviour at the radius, corresponding to the separatrix between the trapped and passing particles. Figure 1 shows post-crash radial profiles of ions having different energies and the same pre-crash profile. For each curve, the particle energy (E) slightly varies with the radius so that the longitudinal adiabatic invariant remains constant. The magnetic moment (μ) is constant along each curve; it is selected so that the trapping parameter (κ) equals to 0.85 at $r = r_{\rm mix}$ (here r is the radial coordinate, $r_{\rm mix}$ is the sawtooth mixing radius, $\kappa^2 = [E - \mu B_0(1-\epsilon)]/(2\mu B_0 \epsilon)$, $\epsilon = r/R_0$, R_0 is the radius of the magnetic axis, $B_0 = B(r=0)$ is the magnetic field). These particles cross the trapped-passing separatrix ($\kappa = 1$) at $r = r_{\rm sep} \approx 0.6 r_{\rm mix}$. The particles with high energies (exceeding the critical energy introduced in [6]) exhibit barrier-type behaviour near the radial coordinate corresponding to the separatrix. The barrier owes its existence to negligible average longitudinal velocity and strong toroidal precession at the separatrix. The passing particles at $r < r_{\rm sep}$ are redistributed due to fast longitudinal motion; the trapped particles, due to resonance [9]. For low-energy particles, the barrier becomes transparent; the energy above which it is important is of the order of the critical energy predicted in [6]. For deeply trapped particles, this barrier is not important, being very close to the magnetic axis; in agreement with [6], these particles are insensitive to sawtooth crashes at super-critical energies.

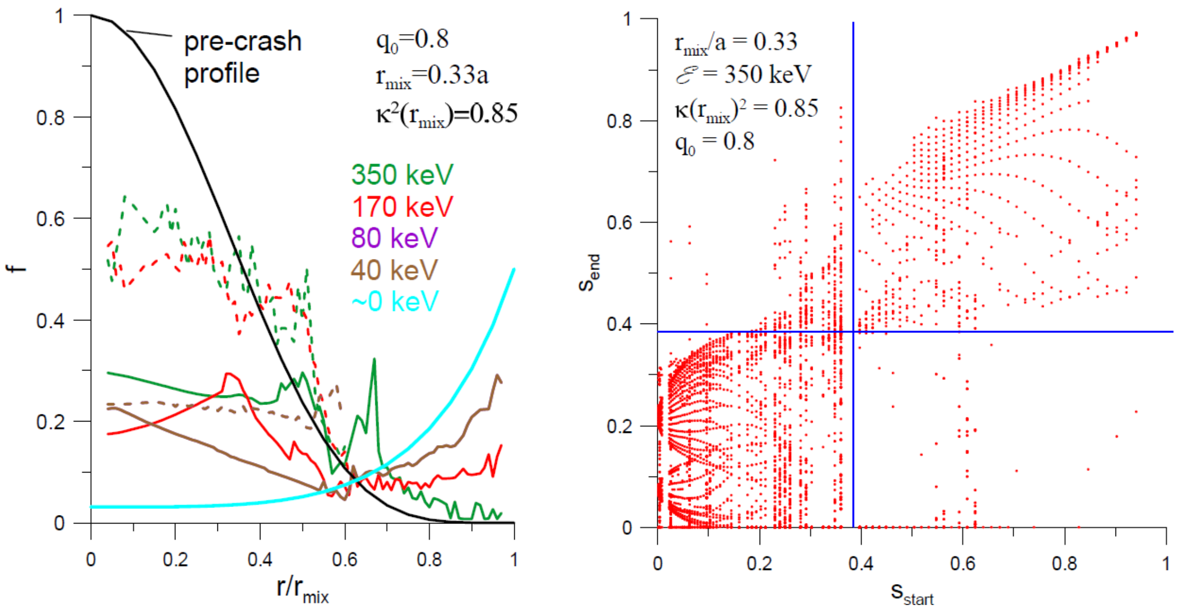

FIG. 1. Redistribution of fast ions. The energies are shown for deuterons in a JET-like tokamak and the sawtooth crash duration of 10^{-3} s. The corresponding energies for α-particles in ITER are about 10 times higher. Left panel: Radial profiles of the distribution function (f) before and after the crash. Solid lines correspond to trapped and co-passing particles; dashed lines, to counter-passing ones. Right panel: Correspondence between the starting and ending points of particle trajectories for 350-keV ions. The blue lines show the position of the separatrix. Notations: q_0 is the central safety factor, κ is the trapping parameter, $s \equiv (r/r_{mix})^2$. High-energy particles weakly penetrate through the barrier at the separatrix.

The results obtained with the OFSEF code were used to develop a rapid code for simulating the sawtooth-induced redistribution of fast ions. The fast-ion redistribution in OFSEF is determined by four dimensionless parameters: the ratio of the crash duration to the precession period (in fact, the properly normalized particle energy), the pitch angle, q_0 (the safety factor at the magnetic axis), and $\epsilon_{\rm mix} = r_{\rm mix}/R_0$. The sawtooth-induced fast-ion mixing can be presented as in integral transformation depending on the mentioned parameters. Results of the OFSEF code are used to find finite-element approximations of the kernels of this transformation at certain mesh points in the parametric space, which are saved in memory. After the kernels are prepared, approximately 10^3 floating-point operations are needed to calculate the post-crash radial profile of the fast ion distribution function (f_{fast}) profile for given pitch angle and energy. A typical example shown in Fig. 2 demonstrates that storing the kernel on a 20×20 radial mesh is sufficient for reaching a sufficient approximation accuracy. Preliminary estimates show that ~ 10^7 numbers are to be stored to reach a reasonable accuracy of interpolation in the parameter space. The numerical part of the code is tested; the interface is being prepared.

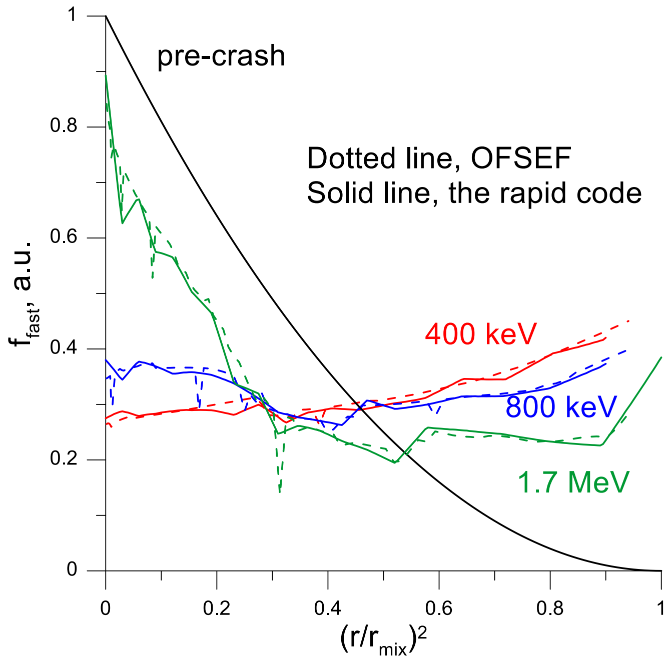

FIG. 2. Comparison of results of the OFSEF code and the new rapid code for passing particles with peaked initial distribution. Notations: black line, pre-crash profile of the fast ion distribution function; colour lines, post-crash profiles for different energies.

3. DETERMINING THE SAWTOOTH CRASH PARAMETERS

The effect of a sawtooth crash on the bulk plasma and the fast ions depends on the spatial extent of the sawtooth mixing, which is characterized by the mixing radius or, alternatively, the inversion radius (the radius separating the regions of the temperature drop and increase during the crash). The crash duration (τ_{crash}) is also an important quantity because it affects the magnitude of the crash electric field. For this reason, according to the theory [6], the critical energy of the trapped ion redistribution is inversely proportional to the crash duration. Thus, knowing the extent and duration of a sawtooth crash is critical for simulations of its effect on fast ions.

Observations of the electron cyclotron emission (ECE) in JET provide data on the evolution of the electron temperature (T_e) with a temporal resolution sufficient to trace the dynamics of a sawtooth crash. The diagnostics measures the emission in the ECE frequency range along a horizontal line of sight located near the magnetic axis. After calibration, 96 frequency channels of the diagnostics provide the temporal evolution of T_e at a set of points located on the line of sight. It is important that the diagnostics does not require tomographic reconstruction. The typical sampling rate is 200 kHz, which is sufficient to trace the dynamics of sawtooth crashes (the typical crash duration is known to be ~10^{-4} s). Unfortunately, the standard calibration procedure employs smoothening to filter the noise (which is rather strong), which reduces the time resolution to ~5×10^{-4} s. For this reason, we took the raw (uncalibrated) signals, filtered them in a different way and used the calibrated signals to find T_e when we needed it.

Two computer codes were developed for determining the inversion radius and the duration of a sawtooth crash.

The code JETSTA (JET SawTooth Analysis) uses matrix median filtering for suppressing the noise. The code analyses all signals in a provided time interval encompassing the crash of interest. The signals are normalized to its smoothened initial values (thus, calibration is avoided). After finding the inversion radius (see Fig. 3), the code determines the crash duration, analysing the average squared deviations ($\Delta(t)$) of the normalized signals from unity. Only the channels inside the inversion radius are included into $\Delta(t)$; the reason for this is that for channels situated near the boundary of the mixing region, it is difficult to distinguish between the crash itself and the heat pulse propagation after the crash. The code analyses the differences of the deviations at adjacent time instants, $\delta(t_i) = \Delta(t_i) - \Delta(t_{i-1})$. It takes as the crash beginning the instant at which $\delta(t_i)$ is much (twice) larger than well before the crash. For the crash end, the code takes the instant at which the relative difference, $\delta(t_i)/\Delta(t_i)$, well exceeds its typical magnitude observed well after the crash. In all analysed cases, this simple strategy permitted the code to select the time interval that one would call "the crash" from physical considerations. Figure 4 shows an example of an atypical crash with three-stage reconnection process and significant post-cursors. The code correctly separates the crash interval from the irregular fluctuations before the crash and post-cursor oscillations after it.

The code DESC (Duration Evaluation of the Sawtooth Crash). Analysis of the structure of the $T_e(t)$-curves. DESC code (Duration Evaluation of Sawtooth Crash) assesses parameters of sawtooth crashes, namely their duration, inversion and mixing radii. The code analyses the temporal evolution of plasma temperature in several spatial locations (see Fig. 5). Because the raw experimental data might contain strong fluctuations, the code filters the data and finds arrays of local maxima and minima of temperature during the period of interest. This makes the code applicable even for data with high divergence. Then, it takes into consideration specific patterns of temperature change, known from Kadomtsev model [10], and looks for this typical behaviour with regards to the radius. For instance, in plasma centre rapid cooling is expected, while in peripheral regions the code looks for corresponding rise of temperature. Thus, comparison of found patterns on different radii creates a comprehensive description of the crash and let the code evaluate its features.

Comparison of results of the two codes is shown in Table 1. Typically, τ_{crash} found by DESC is 1.5 – 2 longer than that found by JETSTA. This is explainable because DESC takes into account the channels located between the inversion radius and the mixing radius. The cases for which the results of the codes differ deserve special analysis.

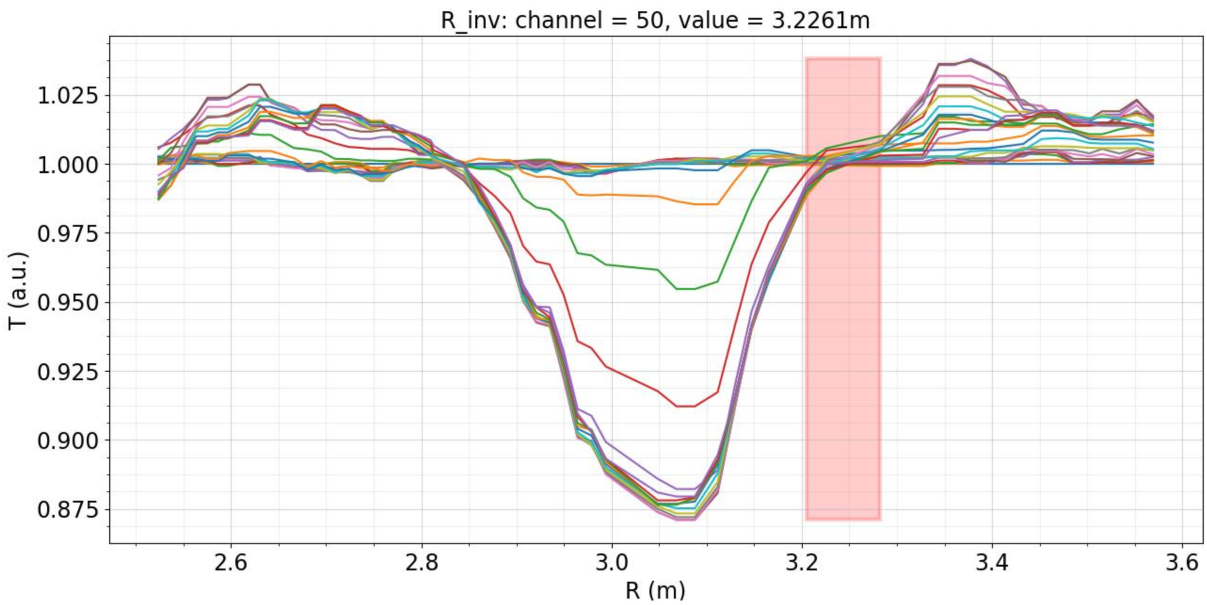

FIG. 3. Determining the inversion radius of a crash in the discharge with the code JETSTA. Shaded region shows the estimated inversion radius. The curves are temperature profiles at various time instants after normalization to the initial profile.

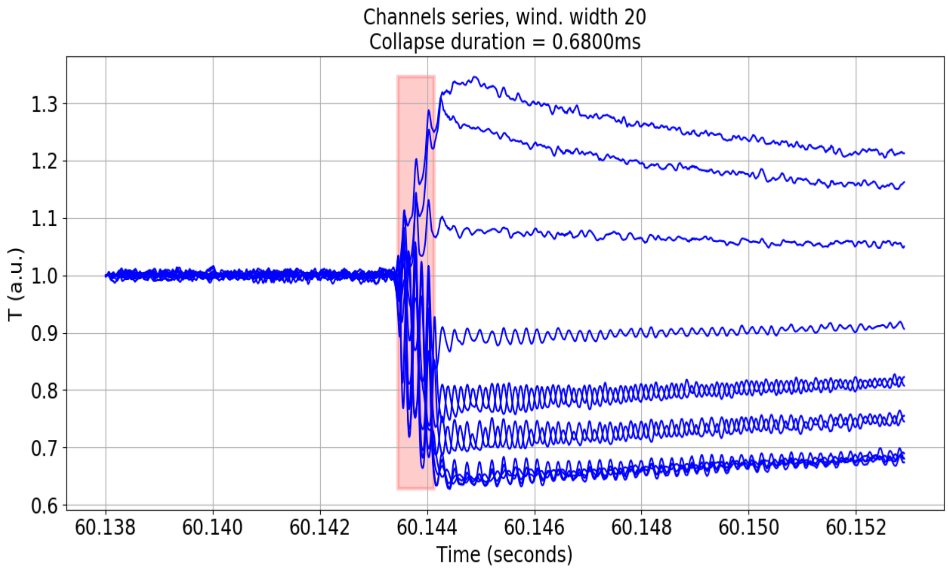

FIG. 4. Determining the crash duration with the code JETSTA. Shaded region shows the estimated time pan of the crash. Curves show the temperature evolution at different points on the line of sight.

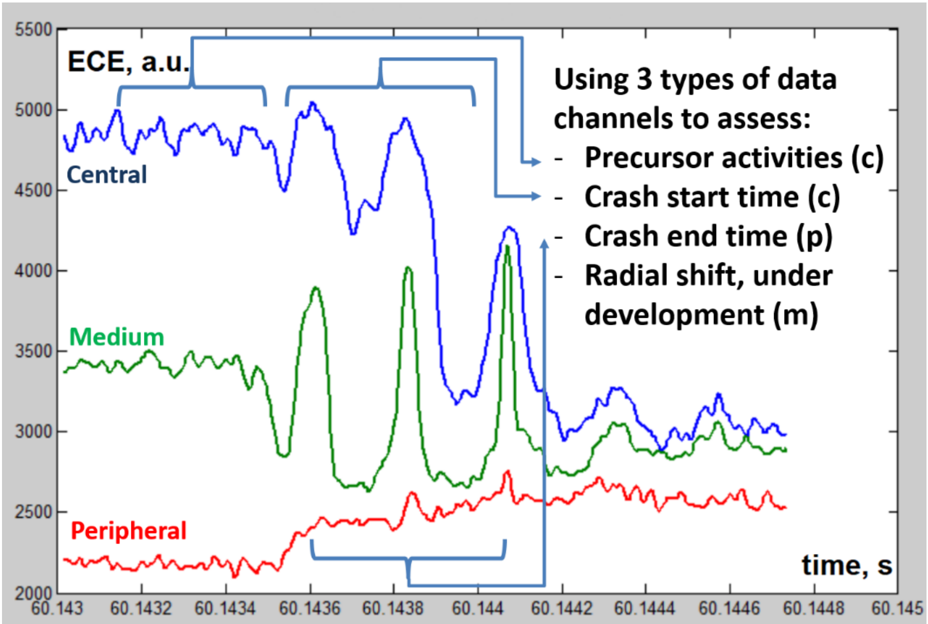

FIG. 5. Determining the crash duration with the code DESC.

TABLE 1. CRASH DURATIONS FOUND BY THE CODES

Sawtooth crash	τ_{crash} (s), DESC	τ_{crash} (s), JETSTA
86459, t = 51.02 s	3.7×10^{-4}	2.6×10^{-4}
86762, t = 51.08 s	1.7×10^{-4}	4.0×10^{-4}
86775, t = 51.41 s	3.9×10^{-3}	2.0×10^{-4}
86774, t = 49.68 s	3.7×10^{-3}	4.9×10^{-4}
92398, t = 48.00 s	1.0×10^{-3}	4.4×10^{-4}
92399, t = 49.27 s	3.1×10^{-3}	2.4×10^{-3}
92400, t = 49.06 s	9.4×10^{-4}	5.6×10^{-4}

92393, t = 49.82 s	5.5×10^{-3}	2.1×10^{-3}

4. SIMULATIONS OF THE REDISTRIBUTION OF ALPHA PARTICLES: EFFECT OF THE SAFETY FACTOR PROFILE

Predictive calculations for ITER demonstrate various shapes of the q-profiles, including flat profiles with a large $q = 1$ radius and "head-and-shoulder" profiles with a small $q = 1$ radius but a wide zone with $q \approx 1$ [11]. To understand how the profile shape affects the redistribution of fast ions, we carried out simulation of redistribution of fusion alpha particles with the OFSEF code, which was recently upgraded to deal with non-parabolic q-profiles. An example of post-crash distributions of trapped and passing alpha particles for a flat q-profile (see Fig. 25 in Ref. [11]) is shown in Fig. 6. The pre-crash profile was taken from Fig. 3 of Ref. [11]. We observe that the redistribution is strong, especially for passing alphas; it results in the formation of hollow radial profiles. The reason is not only in the large magnitude of the $q = 1$ radius. It follows from Kadomtsev's theory [10] that for this specific profile the contribution of the core pre-crash plasma to the post-crash plasma near $r = r_{\text{mix}}$ is larger than for the parabolic profile, which tends to enhance the redistribution of fast ions and the bulk plasma.

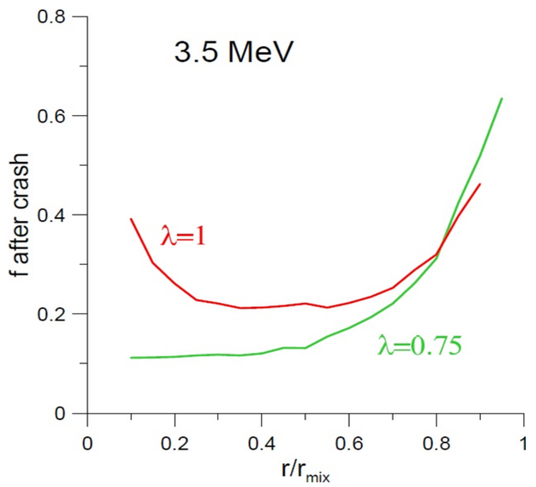

FIG. 6. Post-crash profiles of the distribution function 3.5-MeV alpha particles for a flat q(r)-profile. Green line, passing particles with $\lambda = \mu B_0/E = 0.75$; red line, trapped particles with $\lambda = 1$.

5. SIMULATIONS OF THE EFFECT OF SAWTOOTH CRASHES ON THE NEUTRON EMISSION

The neutron profile monitor in JET provides an opportunity to observe the changes in the spatial distribution of fast deuterium ions, which could be used to verify the existing theories of the sawtooth-induced redistribution of fast ions. As mentioned above, the theory predicts that the passing ions are strongly redistributed at all energies (until the Larmor radius becomes comparable with the sawtooth inversion radius), whereas the trapped particles become insensitive to the crash above some critical energy. In most JET discharges, neutrons are mainly born by deuterons of the NBI (neutral beam injection) beam consisting mainly of passing particles with energies ~100 keV. One can expect that such ions are strongly redistributed. However, in discharges with the third-harmonic D ICRH (ion cyclotron resonance heating), a significant fraction of neutrons is produced by the ICRH tail of trapped deuterons in the MeV energy range [12], which provides an opportunity to verify the theory predictions about the insensitivity of these ions to sawtooth crashes. Therefore, it is of interest to compare the sawtooth effect on the neutron emission in discharges with different ICRH heating schemes with numerical simulations.

To begin with, we selected crashes in discharges #92398–92400 and #86459. In all these discharges there are strong sawtooth events observed when the neutron emission is strong.

Discharges #92398–92400 are hybrid discharges with H minority ICRH, so that most neutrons are produced by DD fusion reactions with participation of NBI-produced fast ions. The neutron emission change caused by the sawtooth event at t = 49.27 s in discharge #92399 is shown in Fig. 7. In addition to the crashes, several weaker events identified as fishbones occur in these discharges; these events result in weak thermal crashes. The thermal crashes that we consider as sawteeth are several times larger.

Discharge #86459 is a third-harmonic D ICRH discharge with relatively high ratio of the ICRH power to the NBI power (3 and 4 MW, correspondingly). Therefore, one can expect that the contribution of the ICRH-accelerated D tail to the neutron emission is significant. Several strong sawtooth crashes occur when ICRH is switched on. The change of the neutron emission due to the crash at t = 51.02 s in this discharge is also shown in Fig. 7.

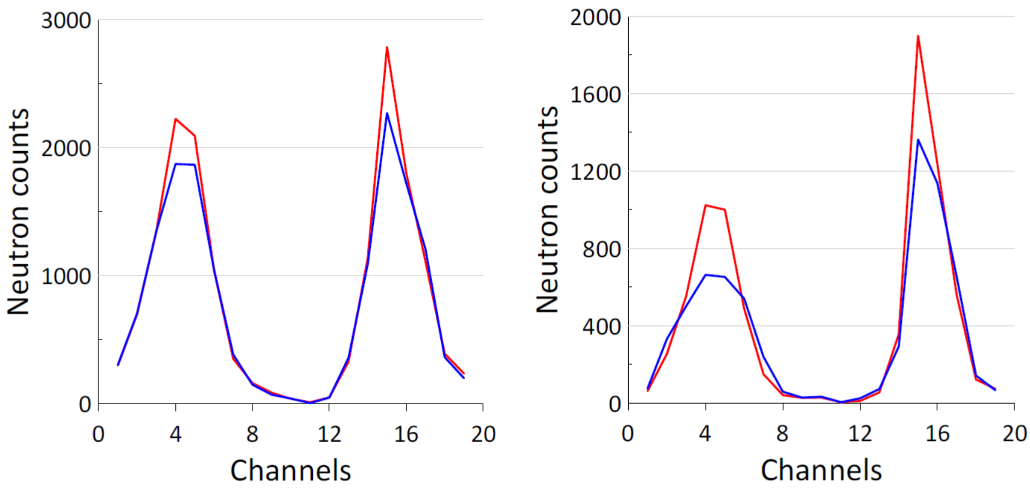

FIG. 8. Change of the signals in the channels of the neutron profile monitor during sawtooth crashes. Left panel, discharge #92399; right panel, discharge #86459; red lines, before the crash; blue lines, after the crash.

The pre-crash distribution function of fast deuterium ions was calculated with the FIDIT Fokker-Planck code [13] for some of the crashes. Trajectories of fast ions during the crashes were calculated with OFSEF. As the radial orbit excursions of MeV deuterium ions are rather large, the guiding-centre version of OFSEF was employed. Now the work on mapping of the phase-space coordinates of the two codes is in progress. After that, the fluxes in the channels of the neutron profile monitor will be simulated.

6. SUMMARY

Simulations of the sawtooth-induced redistribution of fast ions were carried out with the OFSEF code in wide ranges of parameters of the tokamak and the particles. It was found that particles with sufficiently high energies weakly penetrate through the separatrix between the regions of trapped and passing ions. The results of these calculations provided a database for the new rapid code.

Two different codes based on different methods were developed for determining the parameters of a sawtooth crash (the inversion radius and the crash duration) from the data of the ECE diagnostics.

Simulations of the redistribution of fusion alpha particles in ITER were carried out. It was found that the shape of the q-profile can strongly affect the redistribution; in particular, the redistribution is very strong when the q-profile is flat inside the $q = 1$ radius.

Simulations of the effect of sawtooth crashes on the neutron emission are now in progress. The aim of this simulations is to compare the sawtooth effect on fast ion populations produced by different heating techniques, which could provide an opportunity to verify theories predicting the dependence of the redistribution on the energy and pitch angle of fast ions.

ACKNOWLEDGEMENTS

This work has been carried out within the framework of the EUROfusion Consortium and has received funding from the Euratom research and training programme 2014—2018 under grant agreement No 633053 and from the National Academy of Sciences of Ukraine under the Project “Phenomena associated with energetic ions in tokamaks and stellarators.” The views and opinions expressed herein do not necessarily reflect those of the European Commission.

REFERENCES

[1] VON GOELER, S., Studies of internal disruptions and m=1 oscillations in tokamak discharges with soft—X-ray techniques, Phys. Rev. Lett. **33** (1974) 1201.

[2] MEDLEY, S.S., et al., Confined trapped alpha behaviour in TFTR deuterium-tritium plasmas, Nucl. Fusion **38** (1998) 1283.

[3] KIPTILY, V.G., et al., Recent progress in fast ion studies on JET, Nucl. Fusion **49** (2009) 065030.

[4] MUSCATELLO, C.M., et al., Velocity-space studies of fast-ion transport at a sawtooth crash in neutral-beam heated plasmas, Plasma Phys. Control. Fusion **54** (2012) 025006.

[5] JAULMES, F., et al., Numerical and experimental study of the redistribution of energetic and impurity ions by sawteeth in ASDEX Upgrade, Nucl. Fusion **56** (2016) 112012.

[6] KOLESNICHENKO, Ya.I., YAKOVENKO, Yu.V., Theory of fast ion transport during sawtooth crashes in tokamaks, Nucl. Fusion **36** (1996) 159.

[7] NIELSEN, S.K., et al., Fast-ion redistribution due to sawtooth crash in the TEXTOR tokamak measured by collective Thomson scattering, Plasma Phys. Control. Fusion **52** (2010) 092001.

[8] KOLESNICHENKO, Ya.I., LUTSENKO V.V., YAKOVENKO, Yu.V., KAMELANDER, G., Theory of fast ion transport induced by sawtooth oscillations: Overview and new results, Phys. Plasmas **4** (1997) 2544.

[9] KOLESNICHENKO, Ya.I., LUTSENKO V.V., YAKOVENKO, Yu.V., Superbanana orbits and redistribution of marginally trapped fast ions during sawtooth crashes, Phys. Plasmas **5** (1998) 729.

[10] KADOMTSEV, B.B.,

[11] PINCHES, S.D., et al., Energetic ions in ITER plasmas, Phys. Plasmas **22** (2015) 021807.

[12] SALEWSKI, M., et al., MeV-range velocity-space tomography from gamma-ray and neutron emission spectrometry measurements at JET, Nucl. Fusion **57** (2017) 056001.

[13] YAVORSKIJ, V., GOLOBOROD’KO, V., ERIKSSON, L.G. et al., Predictive Fokker-Planck modelling of confined and lost alpha particle in ITER, J. Fusion Energy **34** (2015) 774.